European Polymer Journal 126 (2020) 109563

Contents lists available at ScienceDirect

European Polymer Journal

journal homepage: www.elsevier.com/locate/europolj

Photoinduced properties of "T-type" polyimides with azobenzene or azopyridine moieties

Karolina Bujak[a], Ion Sava[b,*], Iuliana Stoica[b], Vasile Tiron[c], Ionut Topala[c], Rafał Węgłowski[e], Ewa Schab-Balcerzak[d], Jolanta Konieczkowska[d,*]

[a] Institute of Chemistry, University of Silesia in Katowice, Szkolna 9, 40-006 Katowice, Poland
[b] "Petru Poni" Institute of Macromolecular Chemistry, Aleea Gr. Ghica Voda 41 A, Iasi 700487, Romania
[c] Iasi Plasma Advanced Research Center (IPARC), Faculty of Physics, Alexandru Ioan Cuza University of Iasi, Iasi 700506, Romania
[d] Centre of Polymer and Carbon Materials Polish Academy of Sciences, 34 M. Curie-Sklodowska Str., 41-819 Zabrze, Poland
[e] Institute of Applied Physics, Military University of Technology, 2 S. Kalinskiego Str., 00-908 Warsaw, Poland

ARTICLE INFO

Keywords:
Azopolyimides
Surface-relief gratings
LC crystals alignment

ABSTRACT

In this work series of "T-type" polyimides with azobenzene or azopyridine moieties were investigated. It is the first report where the "T-type" polyimides with derivatives of azopyridine were investigated. The *cis-trans* isomerization in the dark in the solid-state was showed. Polyimides with azobenzene derivatives exhibited higher stability of *cis-trans* recovery than their azobenzene analogues. For the inscription of the surface relief gratings, two different intensities of light (10 and 45 mJ/cm^2) and a number of pulses (10 and 100) were used. Polyimides showed the modulation of SRGs up to almost 330 nm. Our studies showed, that azopolyimides are able to orient the nematic liquid crystal molecules in cell-based on effect at the twisted nematic. The obtained maximum value of t_{ON} was 0.9 ms (1 kHz, 1.5 V/μm) for polyimide with azobenzene moieties. Azopolyimides may be successfully used in many photonic devices based on the alignment of the liquid crystal mixture i.e. LC diffraction gratings, Fresnel lens, Vortex, in a photo-pattering technology for creating radical and azimuthal orienting layers.

1. Introduction

Currently, one of the fastest-growing fields of science and technology is photonics. It includes replacing the electron with photon and practical application of its properties in controlling various optical processes [1,2]. Appropriate selection of materials is a key issue in the development of photonics. Photochromic materials, i.e. polymers containing photochromic groups, introduced in the form of permanent, covalently attached structure elements, among which stand out include fulgides, spiropyranes, spirooxazines, diarylethenes or azobenzenes [3–7]. Azopolymers containing azobenzene or azopyridine derivatives are particularly intensely studied [8–11]. They owe their uniqueness to the presence of an azogroup (−N═N−) ensuring the existence of two isomers - *cis* and *trans* [12,13]. During the *trans-cis-trans* photoisomerization reaction of azochromophores under the influence of photon, it occurs a transformation between two spectroscopically different forms of the same compound, leading to a change in physicochemical properties [14,15]. During the transition of a flat *trans*-isomer into the non-flat *cis*-isomer, the molecule gains a dipole moment of 3.0 D, and the distance between the carbon atoms (from 9.0 to 5.5 Å) is changed, that is the geometry of the molecule [16]. Changes in the UV–Vis spectrum that allow following the *trans-cis-trans* isomerization process it also observes. Confirmation of the *trans-cis* conversion is a reduction in the intensity of the band (320 nm) attributed to the transition of the π-π* *trans*-isomer and shifting its maximum absorption towards shorter wavelengths with simultaneous increase of the band intensity (450 nm) of the n-π transition of the *cis*-isomer [16,17]. The molecule then returns to the thermodynamically stable *trans*-isomer as a result of thermal relaxation or as a result of the action of light [7,12,18]. No less important are the physicochemical properties, that the polymeric material characterizes. Polyimides, due to their unique properties, i.e. high glass transition temperature and high thermal stability ensuring the stability of photoinduced anisotropy, as well as the ease of manufacture and wide modifiability of the structure, allow to obtain a product with optimal properties for a given optical process, are particularly popular among scientists [9,19–21]. Because of these advantages, polyimides are used, among others, as an alignment layer for liquid crystals, optical switches, information storage, and processing elements, and for the fabrication of diffractive optical elements [22–25]. Among the mentioned applications, particular importance is

* Corresponding authors.
E-mail addresses: isava@icmpp.ro (I. Sava), jkonieczkowska@cmpw-pan.edu.pl (J. Konieczkowska).

https://doi.org/10.1016/j.eurpolymj.2020.109563
Received 8 October 2019; Received in revised form 6 February 2020; Accepted 10 February 2020
Available online 11 February 2020

attributed to the holographic recording of information, which allows the transition from the two-dimensional form of the storage medium to the spatial recording, as well as the increase of the media capacity and the speed of information processing [26,27].

Azobenzene polymers, due to their light-sensitive properties, are used as materials for the generation of photoinduced optical anisotropy [28,29]. As a result of the interaction of photochromic groups of the polymer with a linearly polarized light, it occurs repeated *trans-cis-trans* isomerization. This causes changes in the angular distribution of the chromophores over time. The consequence of this process is the increase in the number of molecules arranged perpendicular to the electric wavefield intensity vector. The rapid reorientation process causes the increase of photoinduced optical anisotropy (POA), manifested by a change in the refractive index Δn (birefringence), absorption Δα (dichroism) and thickness Δd, leading to the formation of diffraction gratings - amplitude and phase [30–32]. As a result of the microscopic migration of the polymer mass, surface relief gratings (SRG) can be formed [8].

In our previous work, we showed that "T-type" polyimides with *ortho*-substituted azobenzene moieties may exhibit large amplitudes of SRGs up to 440 nm [33]. In work [34] polyimides with azobenzene derivatives attached to the polymer backbone by alkoxy linkage were studied. The photoinduced optical anisotropy in obtained azopolymers was investigated by the holographic recording of a diffraction grating. Polymers showed the first-order diffraction efficiency in the range 0.08–0.23% and modulation of the surface 1–26 nm (Ar^+ laser, λ = 514.5 nm, *p-p* polarization, t = 60 min).

In this work, we present synthesis and characterization of a series of "T-type" polyimides with azobenzene or azopyridine moieties. The results described in our previous works were the motivation for the synthesis of the azopyridine polyimides. We showed that the *cis-trans* isomerization of azopyridine compounds in the dark is significantly faster than azobenzene derivatives [35,36], moreover, side-chain polyimides with derivatives of azopyridine may form higher modulation of SRGs than their azobenzene analogues [34]. The subject of this study is the design of eight new functionalized "T-type" azopolyimides containing imide rings. In this work, two different intensities of light (10 and 45 mJ/cm^2) and a number of pulses (10 and 100) were used for the inscription of SRGs. The modified polyimides presented surface relief modulations with the depth ranging between 15 and 330 nm, depending on the polymer structure and the irradiation conditions. The potential application of azopolyimides as layers for the alignment of the liquid crystals was presented.

2. Results and discussion

The azopolyimides were obtained in one-step polycondensation reaction carried out at high temperature. First, azodiamines, i.e. 2,6-diaminopyridine-2′-methylazobenzene (**AzPy(CH$_3$)**) and 4-[(E)-(pyridin-4-yl)diazenyl]benzene-1,3-diamine (**AzPy**) were obtained in coupling reactions of diazonium salts with 1,3-phenyleniediamine. Azodiamines 2,4-diamino-2′-methylazobenzene (**(Az(CH$_3$)**) and 2,4-diamino-4′-azobenzene (**Az**) has been described before [37–39]. Then, the reaction between synthesized azodiamines with commercial available 4,4′-(4,4′-isopropylidenediphenoxy)-bis(phthalic anhydride) (**EO**) or with previously obtained [40] 2,2′-[N'-phenylethylaniline-di(4-estro-1,2-dicarboxylic)]anhydride (**DB(EtN)**) was carried out to obtain the azo(polyimide)s. The chemical structure of the synthesized polymers was shown in Fig. 1. The polyimides were designed to study the effect of (i) kind of azochromophore (azobenzene/azopyridine) and (ii) chemical structure of the polymer backbone on the thermal *cis-trans* isomerization reaction in the polymer films and formation of the surface relief gratings.

The chemical structures of the newly obtained azodiamines were confirmed by ^{1}H NMR and FTIR spectroscopy and elemental analysis. In ^{1}H NMR spectrum of **AzPy(CH$_3$)**, the signal from the methyl group was observed at 2.49 ppm. For both azodiamines, the amine group signals were present at ~6 ppm. In the FTIR spectra, the presence of NH_2 groups confirm bands in the range of 3498–3200 cm^{-1}. The absorption bands at 1616 and at around 1584 cm^{-1} are due to stretching deformations in the aromatic rings (−C═C−) and in azolinkages (−N═N−), respectively. The band characteristic of the pyridine ring was found at about 1000 cm^{-1}. In addition, the absorption of C−H units in the methyl group in **AzPy(CH$_3$)** was present at 2976 cm^{-1}. Elemental analysis exhibited good agreement with the calculated contents of nitrogen, hydrogen, and carbon. The UV–Vis absorption spectra of the obtained azodiamines were characterized by the occurrence of two absorption maxima attributed to the π-π* (about 280 nm) and the n-π* transitions (about 430 nm). The melting point of the obtained compounds was higher than 187 °C.

2.1. Polymer characterization

The chemical structures of the polyimides were characterized by instrumental techniques including FTIR and ^{1}H NMR spectroscopies and also by means of elemental analysis. The FTIR spectra of the polyimides clearly showed strong absorption in the range of 3093–2838 cm^{-1}, due to the stretching vibration of C−H in ethyl and methyl groups. The absorption bands at about 1780 cm^{-1} and 1725 cm^{-1} are attributed to the asymmetric and symmetric stretching vibration of the carbonyl group in the five-membered imide ring. Moreover, all of the studied polyimides showed absorption bands at ~1350 cm^{-1} and in the range of 744–723 cm^{-1} correspond to the −C−N− stretching and deformation vibration of the imide ring respectively. The polyimides showed an absorption band approximately at 1600 cm^{-1} and a range of 1252–1236 cm^{-1} corresponding to the vibration of the azobenzene moiety (−N═N−) and ether linkages −C−O−C− respectively. The band at about 1000 cm^{-1} was characteristic of polymers containing pyridine ring in their structure (**PI-AzPy-1**, **PI-AzPy-2**, **PI-AzPy-3**, **PI-AzPy-4**). The presence of an additional broad band in the range of 3549–3209 cm^{-1} was characteristic of polymers with ester linkages in the main chain (**PI-AzPy-1**, **PI-AzPy-3**, **PI-Az-1, and PI-Az-3**). The ^{1}H NMR spectra of the polyimides showed a signal at 1.70 ppm corresponding to the methyl groups and at about 3.85 and 4.50 ppm corresponding to the ethyl groups located in the dianhydride part. In ^{1}H NMR spectrum of polyimides prepared from **Az(CH$_3$)**, a signal at 2.61 ppm typical for a methyl group was observed. The signals in the range of 6.35–8.72 ppm correspond to the aromatic rings.

Wide-angle X-ray diffraction measurements show the submolecular structure of polyimides. All tested materials exhibited the same diffraction patterns characteristic for amorphous materials with one broad diffraction peak of diffusion type centered at 22° (2θ). X-ray diffraction patterns are shown in Fig. 2.

The reduced viscosity (η_{red}) of all synthesized polyimides was ca. 0.1 dL/g, as shown in Table 1. The obtained values suggest rather low molar masses of polymers. Nevertheless, despite the low molecular weights, all the obtained azopolymers exhibited good film-forming properties on the glass substrate. The solubility properties of the obtained azopolymers were determined qualitatively by dissolving 10 mg powdered polyimides samples in 1 ml of organic solvent (at room temperature and at the boiling point of the solvent). The results are given in Table 1. All azopolymers were excellent soluble at room temperature in polar solvents, i.e. NMP and DMF. In addition, some polyimides were easily soluble in polar DMSO, low-boiling-point solvents such as THF, chlorinated solvent - $CHCl_3$ and cyclohexanone. Good solubility of the obtained polymers resulted from the presence of ester and ether groups in the main chain, which contribute to the improvement of solubility [38,42] and probably low molar masses. Polyimides with pyridine rings in azo units (**PI-AzPy-3**, **PI-AzPy-4**) exhibited the worst solubility in THF, cyclohexanone, and $CHCl_3$ compare to other azopolyimides.

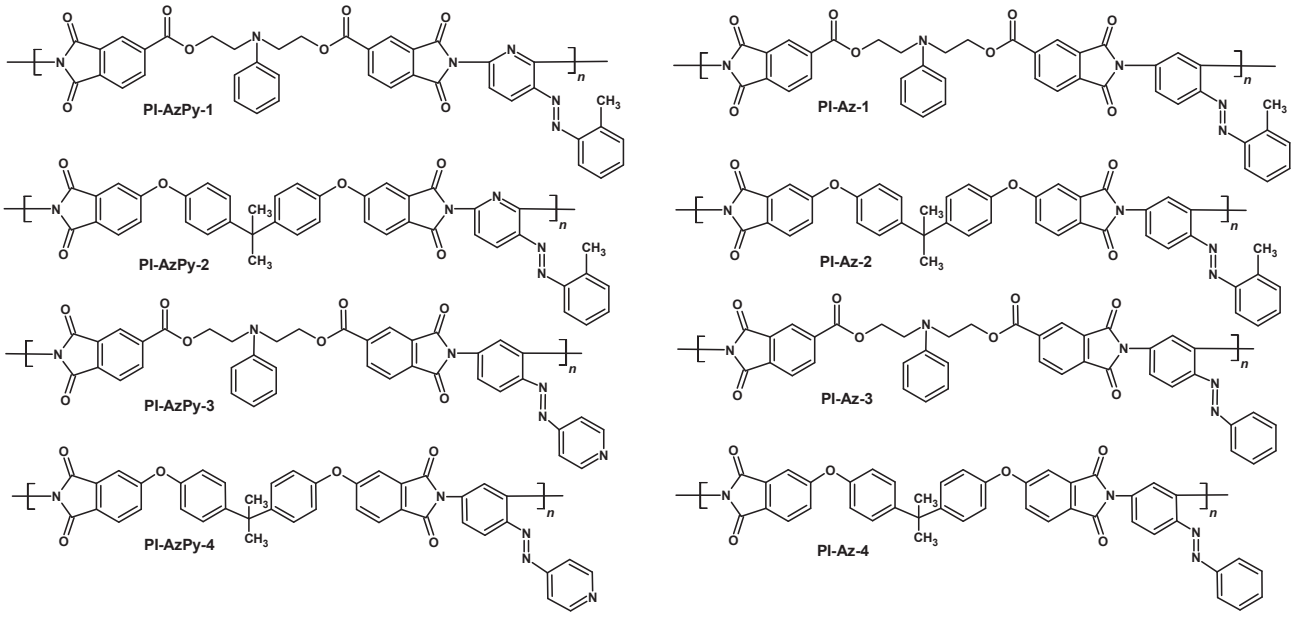

Fig. 1. Chemical structures of the synthesized azopolyimides.

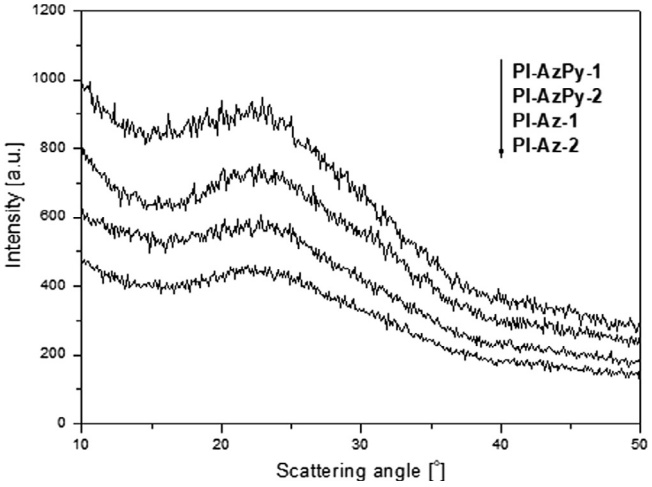

Fig. 2. X-ray diffraction patterns of the azopolyimides.

Table 1
The reduced viscosity and solubility of polyimides.

Polymer code	η_{red} (dL g^{-1})[a]	Solubility[b]					
		DMF	DMSO	THF	$CHCl_3$	Cyclohexanone	NMP
PI-AzPy-1	0.2	+	+	+	+	+	+
PI-AzPy-2	0.2	+	+	+	+	+	+
PI-AzPy-3	0.1	+	+	±	±	±	+
PI-AzPy-4	0.1	+	+	±	±	±	+
PI-Az-1	0.1	+	+	±	±	+	+
PI-Az-2	0.1	+	+	+	+	+	+
PI-Az-3 [40,41]	0.1	+	+	+	+	+	+
PI-Az-4	0.1	+	+	+	+	+	+

Symbols: + soluble; ± partially soluble on heating.
Solvents: DMF – dimethylformamide, DMSO – dimethyl sulfoxide, THF – tetrahydrofuran, $CHCl_3$ – chloroform, NMP – N-methyl-2-pyrrolidone.
[a] Reduced viscosity of the polymers dissolved in NMP, concentration = 0.03 g/100 ml at temperature 25 °C.
[b] The qualitative solubility was tested with 10 mg samples in 1 ml of solvent.

The optical properties of azopolymers were analyzed by UV–Vis spectroscopy in both in NMP solution and in the solid-state as thin-film cast on a glass substrate. The spectral range of UV–Vis measurements was limited by the transparency of the used solvent and the substrate. The values of the maximum absorption band (λ_{max}) of polyimides in the NMP solution and in the film are summarized in Table S1. UV–Vis absorption spectra of polyimide solutions in NMP showed similar features. For the polymers with azobenzene moieties in the structure, two characteristic absorption bands were observed. The band located at around 330 nm was attributed to the transitions of the π-π* whereas the transitions of n-π* corresponded to the weak band at around 450 nm [17]. Absorption spectra for azopolyimides in NMP solution and polymer film are collected in Fig. 3. Comparison of UV–Vis absorption spectra of solutions and polyimide films showed the same shape of absorption bands. Incorporation of a nitrogen atom to the chromophore results in a change of the absorption spectra in comparison to the polyimides with azobenzene chromophore.

2.2. Thermal properties

The thermal behavior of prepared azopolymers ie. glass transition temperatures (T_g) and thermal stability were examined by a differential scanning calorimetry (DSC) and thermogravimetric analysis (TGA) in an inert gas atmosphere - nitrogen. The results of the measurements are summarized in Table 2.

It is obvious that the thermal properties depend on the chemical structure of the materials, in this case on the architecture of the dianhydride and azodiamine used for synthesis. Glass transition temperatures determined by the midpoint of the baseline shift of the polymers were in the range of 145–228 °C (Table 2). Considering the chemical structure of the polymer main chain it was found that poly(ether imide)s showed the higher T_g values (173–228 °C) compared to poly(ester imide)s (145–165 °C). This may be due to the increased stiffness of the polymer backbone with ether groups. In our previous work, we showed that the presence of ether groups in the polymer backbone increases the stiffness of the polymer backbone compared to the ester linkages [43,44]. Comparing the polymers obtained from the same dianhydride, it was found that incorporation of the azopyridine with nitrogen in the side chain of the polymer backbone increase the T_g of the polyimides (**PI-AzPy-3**, **PI-PyAz-4**), while derivative of azobenzene with no substituent (**PI-Az-3**, **PI-Az-4**) decrease the T_g as compared to the other

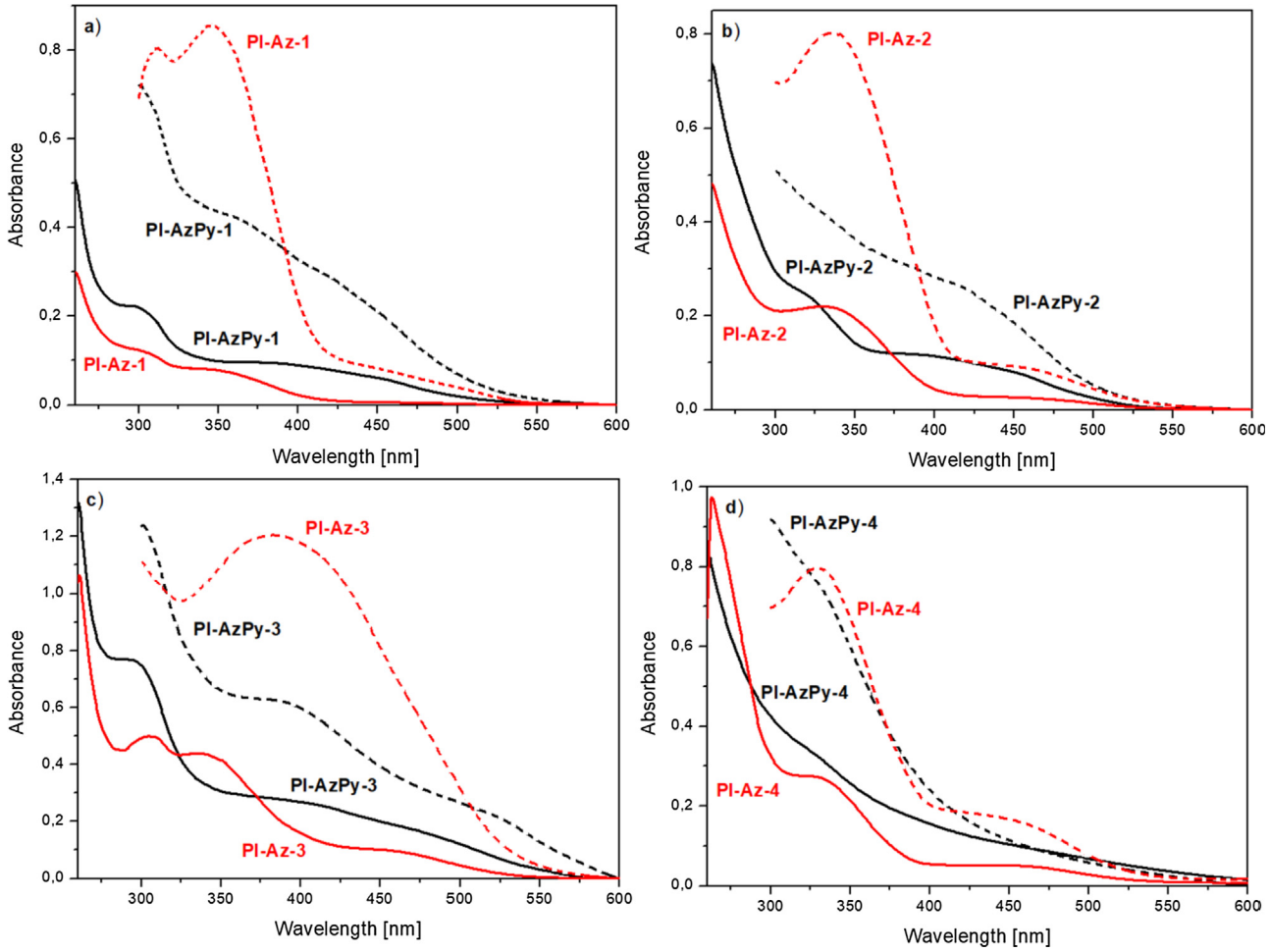

Fig. 3. UV–vis spectra of azopolyimides in NMP solution (solid line) and polymer film (dot line) for polyimides (a) **PI-Az-1/PI-AzPy-1**, (b) **PI-Az-2/PI-AzPy-2**, (c) **PI-Az-3/PI-AzPy-3**, and (d) **PI-Az-4/PI-AzPy-4**.

Table 2
Thermal properties of the investigated polyimides.

Polymer code	DSC	TGA			
	T_g (°C)	T_5 (°C)[a]	T_{10} (°C)[b]	T_{max} (°C)[c]	Residual weight (%)[d]
PI-AzPy-1	157	327	361	405; 696	43
PI-AzPy-2	182	359	414	376; 533	51
PI-AzPy-3	165	248	298	360; 534	40
PI-AzPy-4	228	371	431	462; 544	50
PI-Az-1	161	329	365	343; 411; 618	51
PI-Az-2	188	433	494	381; 531	41
PI-Az-3 [40]	145	303	325	309; 376	37
PI-Az-4	173	447	489	477; 540	55

[a] Decomposition temperature of 5% weight loss.
[b] Decomposition temperature of 10% weight loss.
[c] Temperature of the maximum decomposition rate by DTA.
[d] Residual weight at 800 °C in nitrogen.

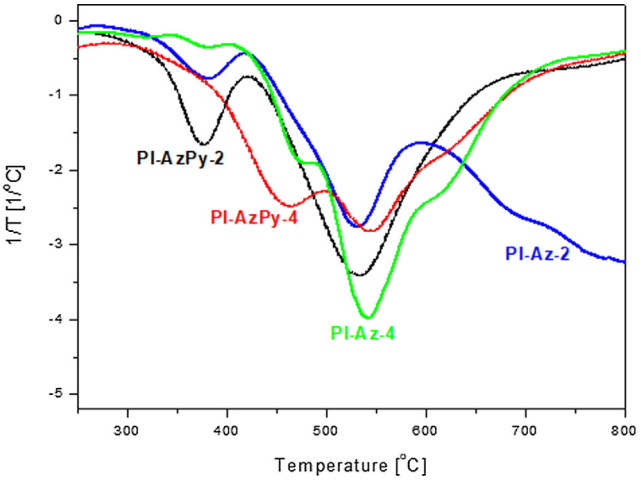

Fig. 4. DTG curves of azopolyimides.

polymers.

Considering criteria determining thermal stability, such as the temperature of 5% (T_5) and 10% (T_{10}) weight loss and temperature of the maximum of polymer degradation rate (T_{max}), it can be concluded that the tested azopolymers showed good thermal stability. The temperatures of T_5 and T_{10} as the beginning of the thermal decomposition of material were in the range of 248–447 °C and 298–494 °C, respectively (Table 2). Lower thermal stability compared to more conventional polyimides (decomposition temperatures above 450 °C) may result from the presence of thermally labile azobonds [45]. Azopolymers with a covalently attached chromophore generally show two or three degradation steps [46]. The first and second, in the range 309–477 °C was related to the thermal degradation of the azogroups, while the third stage in the temperature range 376–696 °C represented the decomposition of the polymer main chain [47,48]. Representative differential thermogravimetry curves (DTG) for selected polyimides are presented in Fig. 4. Residual weigh of the tested polyimides at 800 °C

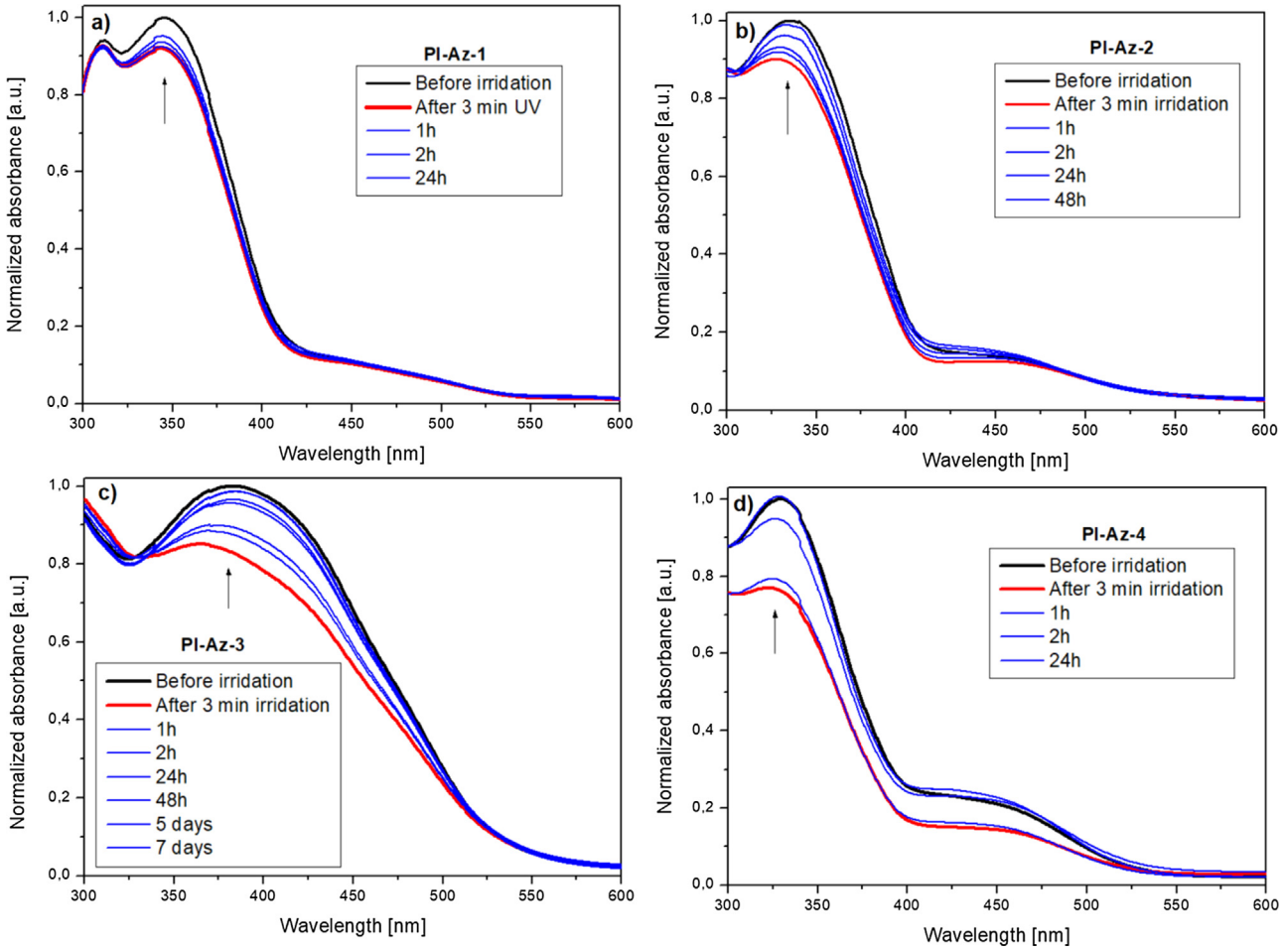

Fig. 5. UV–Vis absorption spectra of the polyimides with azobenzene moieties monitored for thin films. Absorption spectra were registered before irradiation (black spectra) and after 3 min irradiation with a 9 W continuous-mode diode (405 nm) (red spectra) and during *cis-trans* isomerization within 1 h–7 days. (For interpretation of the references to colour in this figure legend, the reader is referred to the web version of this article.)

were in the range of 37–55%. The influence of the chemical structure on the thermal stability of the azopolymer was observed. Similar to in the case glass transition temperatures, poly(ether imide)s characterized higher thermal stability than poly(ester imide)s with the same azo chromophore. Considering the kind of attached azo derivative, higher thermal stability was observed for polyimides with pyridine ring in the side chain or azobenzene with a CH_3 group than polyimides with azobenzene moieties without substituents (cf. Table 2).

2.3. *Cis-trans isomerization reaction*

The dark *cis-trans* isomerization of azopolymers was monitored in the solid-state as a thin film on a glass substrate. All studied polymers exhibited the absorption region in the range of 300–570 nm. The maximum of the absorption of the polyimide with azobenzene moieties was clearly seen (Fig. 5), while the maximum of the polymers with derivatives of azopyridine was not well-formed (Fig. S2). Because of that, the content of the *cis*-isomer after irradiation was evaluated only for polymers with azobenzene derivatives. Before exposure to the excitation beam, the absorption spectra of polyimides with azobenzene moieties were characterized by one, two or three absorption bands varying in intensity, attributed to the transitions of π-π* *trans*-isomers, and corresponded to 100% of the *trans*-isomer content in the sample (Table 3). The *cis–trans* isomerization process was studied for polymers after exposure to UV radiations from a 9 W lamp working at a wavelength of 405 nm. The excitation light-induced both π-π* and n-π* transitions for all polyimides. The photostationary state was achieved after 3 min of irradiation. The *trans-cis* isomerization was confirmed by the reduction of the λ_{max} intensity and the shift towards shorter wavelengths (red lines in Fig. 5). The largest shift of maximum absorption was observed for **PI-Az-3**. After turning off the excitation beam the thermal *cis-trans* return of azosystems to the initial state was observed. Changes in the absorption spectrum were monitored within 1 h–7 days. UV–Vis spectra of thermal *cis–trans* back reaction for azopolyimides with azobenzene moieties and for polymers with azopyridine derivatives are shown in Fig. 5 and Fig. S2, respectively.

Table 3
Maximum absorption of the *trans*- and *cis*-isomers in the solid state, and content of *cis*-isomer obtained directly after 3 min of irradiation and after 24 h of relaxation for azopolyimides, except **PI-AzPy-4**.

Polymer code	λ_{max} of the *trans*-form [nm]	λ_{max} of the *cis*-form [nm]	Content of *cis*-isomer [%]	
			After 3 min of irradiation	After 24 h of relaxation
PI-Az-1	312; 346; 450	311; 343; 445	8	5
PI-Az-2	335; 445	327; 441	11	4
PI-Az-3	383	366	17	4
PI-Az-4	330; 431	322; 424	24	0
PI-AzPy-1	327*; 399*; 561*	328*; 402*; 575*	6.3	4
PI-AzPy-2	356*; 548*	360*; 556*	10	4
PI-AzPy-3	341*; 468*	341*; 463*	3.5	0.6

After turning off the UV-lamp, the changes in absorbance were observed for all azopolyimides, except for **PI-AzPy-4** (Fig. S2). The content of *cis*-isomer directly after UV-irradiation and after 24 h of *cis-trans* relaxation was determined according to eq. 1 (cf. Support. Inf.), and the results are collected in Table 3. Considering the kind of azo-compound more stable isomerization was observed for polymers with azobenzene derivatives. The full recovery to *trans*-form was observed within 24 h–7 days, while polyimides with azopyridine moieties relaxed within 24 h (Table 3). The observation was similar to the results described in the literature. The *cis-trans* isomerization in solution was faster for azopyridine compounds than derivatives of azobenzene [33,49]. We calculated that the conversion of the *trans*- to *cis*-isomer for polyimides with an azobenzene derivative immediately after 3 min exposure to the UV lamp is more efficient for polymers with ether linkages than from ester groups and decreases in order **PI-Az-4** > **PI-Az-3** > **PI-Az-2** > **PI-Az-1**. The most efficient *trans-cis* isomerization was observed for **PI-Az-4.**, where after 3 min of irradiation 24% of *cis*-isomer was generated (Table 3). Despite the highest content of *cis*-isomer, **PI-Az-4** characterized fast return to *trans*-form. After 24 h the full recovery was observed. The result may be connected with the applied wavelength of the excitation beam. A source of excitation light (405 nm) was close to the maximum absorption of the **PI-Az-3**, not like for the other polyimides (**PI-Az-1**, **PI-Az-2,** and **PI-Az-3**) on its slope.

2.4. Surface relief gratings

Atomic force microscopy highlighted the generation of the surface relief gratings, induced by UV laser irradiation, on the surface of all azopolymer films, both in the case of polyimides containing azobenzene with CH_3 group or without any substituent and in the case of polyimides with pyridine rings attached to polymer backbone or with pyridine in the side chain. However, their appearance depends on the polymer structure, its isomerization capacity and irradiation conditions (energy fluency and the number of pulses). In order to indicate if the investigated surfaces have a particular orientation or not, the texture direction index of the surface (Stdi) was examined by analyzing the 3D AFM height images and the corresponding angular spectra. This tridimensional roughness parameter shows the degree of surface orientation and can be defined as the ratio of the average amplitude sum (over angle α), $A(\alpha)$, to its maximum, A_{max} (amplitude sum of the dominating direction), by the equation:

$$Stdi = (1/M) \sum_{j=0}^{M-1} A(\pi j/M)/A_{max}$$

where M is the number of equiangular separated radial lines which are drawn at angles $\alpha = \alpha_j = \pi j/M$ ($j = 0, 1,\ldots, M-1$) from the central point of the Fourier spectrum image [50].

If the amplitude sum of all directions is almost similar, the values of the Stdi parameter will be close to 1 and so the samples will have no preferential orientation. In other words, the surface will present isotropic morphology. Instead, if Stdi values will be close to zero, this will indicate a dominant direction (anisotropy) of the morphology. Also, the fast Fourier transform (FFT) results of the corresponding AFM images clearly confirmed the periodic structured pattern on the surface [51,52]. Besides the texture direction index of the surface, the root means square roughness (Sq), calculated from the AFM images, was also displayed in Table 4. Representative 2D AFM images, corresponding cross-section profiles and fast Fourier transform (FFT) images of the SRGs obtained for selected azopolyimides are shown in Fig. 6a-d, and Fig. 7a-d.

At lower energy density and number of pulses (10 mJ/cm^2 and 10 pulses), SRGs begin to form with pitch values of the same order of magnitude as that of the phase mask. Some of them were uniform and well-defined, as was the case of polyimides synthesized from more flexible dianhydride, namely **DB(EtN)** with azobenzene or azopyridine moieties. This was confirmed by the low values obtained for Stdi, namely 0.585 for **PI-AzPy-1**, 0.211 for **PI-AzPy-3,** 0.394 for **PI-Az-1** and 0.138 for **PI-Az-3**. The nanostructures obtained for the sample **PI-Az-3** with the highest anisotropy of morphology, given the lowest value of the texture direction index, are exemplified in Fig. 6a. The inset FFT-image form Fig. 6a shows a higher order of the surface structures. Other SRGs were barely visible, especially for the samples synthesized from the less flexible dianhydride **EO**, with azobenzene or azopyridine moieties. Still, the values of the texture direction index indicate a dominant direction of the morphology (0.706 for **PI-AzPy-2**, 0.411 for **PI-AzPy-4**, 0.478 for **PI-Az-2** and 0.714 for **PI-Az-4**). In Fig. 6b has presented the sample with the highest Stdi, namely **PI-Az-4**, in which case the self-organization just begins to produce at 10 mJ/cm^2 and 10 pulses. Taking into consideration that the structuring looks very weak, the inset FFT-image leads to rather randomly distributed bump patterns.

As the number of pulses increases to 100, the structuring becomes more visible and higher. In particular cases (polyimides **PI-AzPy-3** (Fig. 6c) and **PI-AzPy-4** (Fig. 6d) with pyridine rings in azo units), the azopolymers, under the photofluidization process, spontaneously form nanodomes by creeping and aggregation, which then attaches itself to adjacent ones, resulting regularly oriented nanogratings. These nanogratings were very well defined, especially for **PI-AzPy-4**, a fact confirmed by the values of Stdi (0.233 and 0.322, respectively). The aspect of the inset FFT-image obtained for **PI-AzPy-4** (Fig. 6d) indicates that the repetitive structures are identical and there are no additional structures between them, as it happens in **PI-AzPy-3** case (Fig. 6c).

When the samples were nanostructured using a higher energy density of 45 mJ/cm^2 and 10 pulses of irradiation, the nanogrooves were increasingly differentiated. Their widths, estimated from the obtained height profiles, for example, using the representative 2D AFM images displayed in Fig. 7a and Fig. 7b for **PI-Az-2** and **PI-Az-4**, respectively, were of about 500 nm. The ridges of the ordered nanostructures were smooth, without any additional structuring. Analyzing these two samples and the corresponding FFT-images, it can be observed for the polyimide **PI-Az-2,** containing, in addition to polyimide

Table 4
The surface roughness parameters (Sq-root mean square roughness and Stdi-surface texture direction index) calculated from the AFM images and Fourier spectrum.

Sample/energy density/number of pulses	Surface roughness parameters		Sample/energy density/number of pulses	Surface roughness parameters	
	Sq (nm)	Stdi		Sq (nm)	Stdi
PI-AzPy-1/10/10	21.6	0.585	**PI-Az-1/10/10**	2.6	0.394
PI-AzPy-1/10/100	67.6	0.435	**PI-Az-1/10/100**	22.3	0.439
PI-AzPy-1/45/10	29.7	0.242	**PI-Az-1/45/10**	16.9	0.335
PI-AzPy-1/45/100	81.8	0.663	**PI-Az-1/45/100**	82.1	0.641
PI-AzPy-2/10/10	28.4	0.706	**PI-Az-2/10/10**	3.9	0.478
PI-AzPy-2/10/100	13.6	0.758	**PI-Az-2/10/100**	31.5	0.608
PI-AzPy-2/45/10	51.4	0.429	**PI-Az-2/45/10**	32.4	0.314
PI-AzPy-2/45/100	33.1	0.567	**PI-Az-2/45/100**	62.8	0.649
PI-AzPy-3/10/10	5.5	0.211	**PI-Az-3/10/10**	19.8	0.138
PI-AzPy-3/10/100	36.3	0.233	**PI-Az-3/10/100**	70.7	0.472
PI-AzPy-3/45/10	51.3	0.471	**PI-Az-3/45/10**	87.5	0.552
PI-AzPy-3/45/100	123.5	0.467	**PI-Az-3/45/100**	127.4	0.373
PI-AzPy-4/10/10	2.3	0.411	**PI-Az-4/10/10**	5.6	0.714
PI-AzPy-4/10/100	50.9	0.322	**PI-Az-4/10/100**	74.2	0.444
PI-AzPy-4/45/10	46.3	0.592	**PI-Az-4/45/10**	29.8	0.282
PI-AzPy-4/45/100	53.9	0.478	**PI-Az-4/45/100**	101.3	0.559

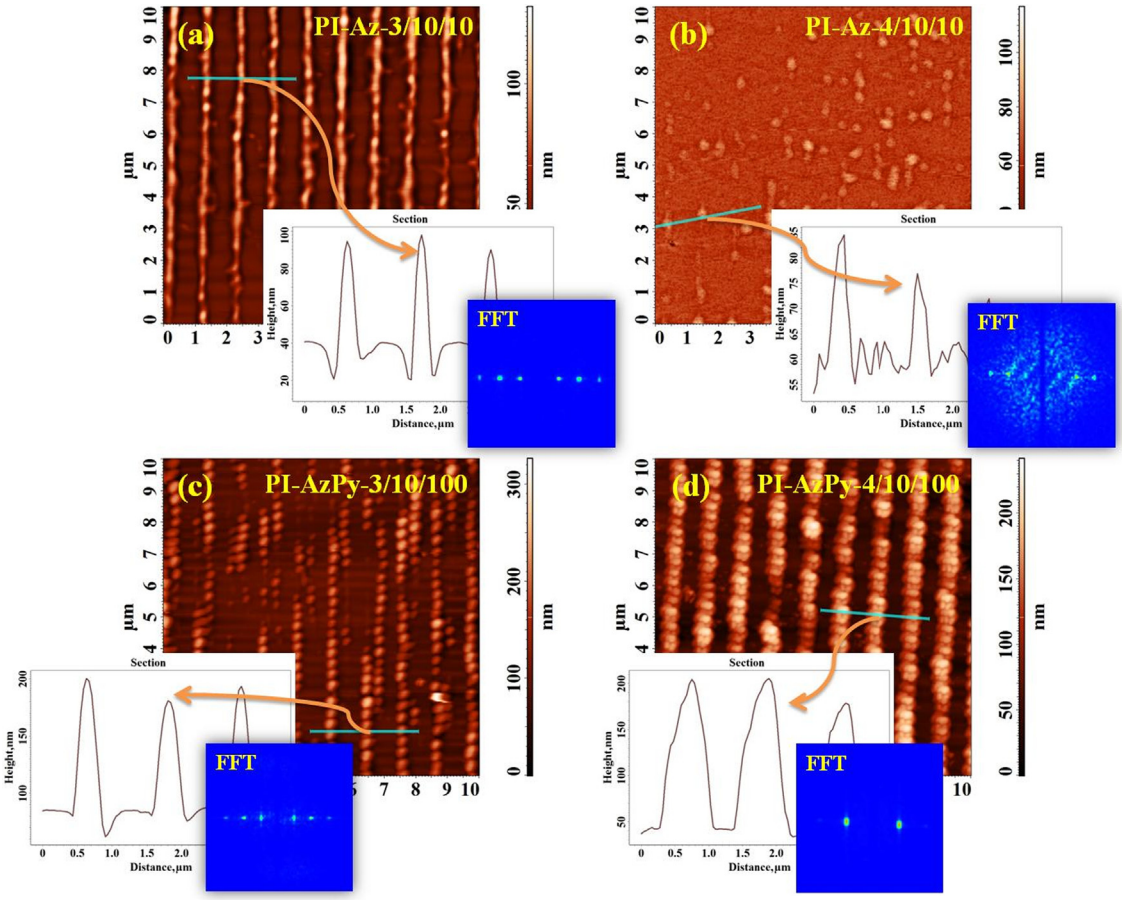

Fig. 6. Representative 2D AFM image, corresponding cross-section profiles, and fast Fourier transform (FFT) images of the SRGs obtained for (a) **PI-Az-3** and (b) **PI-Az-4** at 10 mJ/cm^2 and 10 pulses and for (c) **PI-AzPy-3** and (d) **PI-AzPy-4** at 10 mJ/cm^2 and 100 pulses.

PI-Az-4, the azobenzene with CH_3 groups, the appearance of weakly visible secondary nanogrooves, probably due to the interference of the ± 1 diffraction orders. This increases also the value of Stdi to 0.314, comparing to **PI-Az-4** polyimide (0.282). Instead, for **PI-Az-4**, the FFT-image denotes identical repeating patterns, having no supplementary structures among them. When 100 pulses of irradiation were used, the widths of the SRGs were increasing and in some regions, these structural formations extend in such manner that they tend to overlap, with significant loss of their borders. Therefore, in these cases, the SRGs were not so well-defined, the morphology slightly tending to lose its anisotropy, as indicated by the built FFT-images. This fact was also confirmed by the calculated Stdi, which, for all the samples was greater than 0.45, but not exceeding 0.65. Likewise, it was observed that the or donated structures had globular form only in the cases of polyimides with methyl groups substituents in azobenzene units, with (**PI-AzPy-1** and **PI-AzPy-2**) or without pyridine in the main chain (**PI-Az-1** and **PI-Az-2**), regardless the dianhydride structure. The Fig. 7c is presented a representative 2D AFM image of the SRGs obtained in this case for **PI-AzPy-2.** For the rest of the samples, the surface topography of the nanogrooves tends to become sharpen and hone, as can be observed in Fig. 7d for **PI-AzPy-4**.

As a general observation, valid for all the samples, it can be stated that, for the same energy density, whether high or small, the higher the number of pulses, the more higher heights will have the formed surface relief gratings, inducing in the same time the increasing of the root mean square roughness, as seen in Table 4 (excepting the **PI-AzPy-2** sample). When 10 pulses of irradiation were used, the surface relief gratings have a relatively smooth appearance, their widths increasing as the energy increases. Hierarchical multiscale surface relief gratings appear only in the cases where a greater number of pulses of irradiation were used, and they are even more complex as the energy increases. These phenomena can be explained taking into consideration that two parallel mechanisms of nanostructuration can occur. As previously shown [53], the first one is responsible for the material photo-fluidization induced by the *trans-cis* isomerization process of the azo-segments, and the second one is responsible for the azobenzene dipoles orientation, having effects in supramolecular re-organization processes. It is difficult to appreciate the contribution of each mechanism, but it seems that when the first mechanism was dominant (at 10 pulses of irradiation), the induced pattern was more organized and compacted, and when the chains re-ordering mechanism was prevalent (at 100 pulses of irradiation), the morphology of the induced pattern was much more complex. None of the models concerning the azo-polymers surface nanostructuration mechanisms proposed until now completely explain the surface relief formation; however, a consensus has been reached: the azobenzene dipoles orientation probably induce o more organized and compacted structure, having, as a result, a material contraction in the light-exposed regions, generating the grooves in the dark areas [53]. Thus, the highest intensity of the interference pattern corresponds to the valley of SRG, as resulted from the cross-section profiles, due to the mass transport effect [54-56].

2.5. Alignment of the liquid crystals

As to test the ordering properties of **PI-Az-4** thin films, the observation of an electro-optical effect at the twisted nematic (TN) was selected. At the TN electro-optical effects, the unidirectional (aligned) molecular anchoring at the boundary surface is the main factor of the induction of the TN structure and moreover plays an important role at recovering the twisted structure after removing of the driving electric

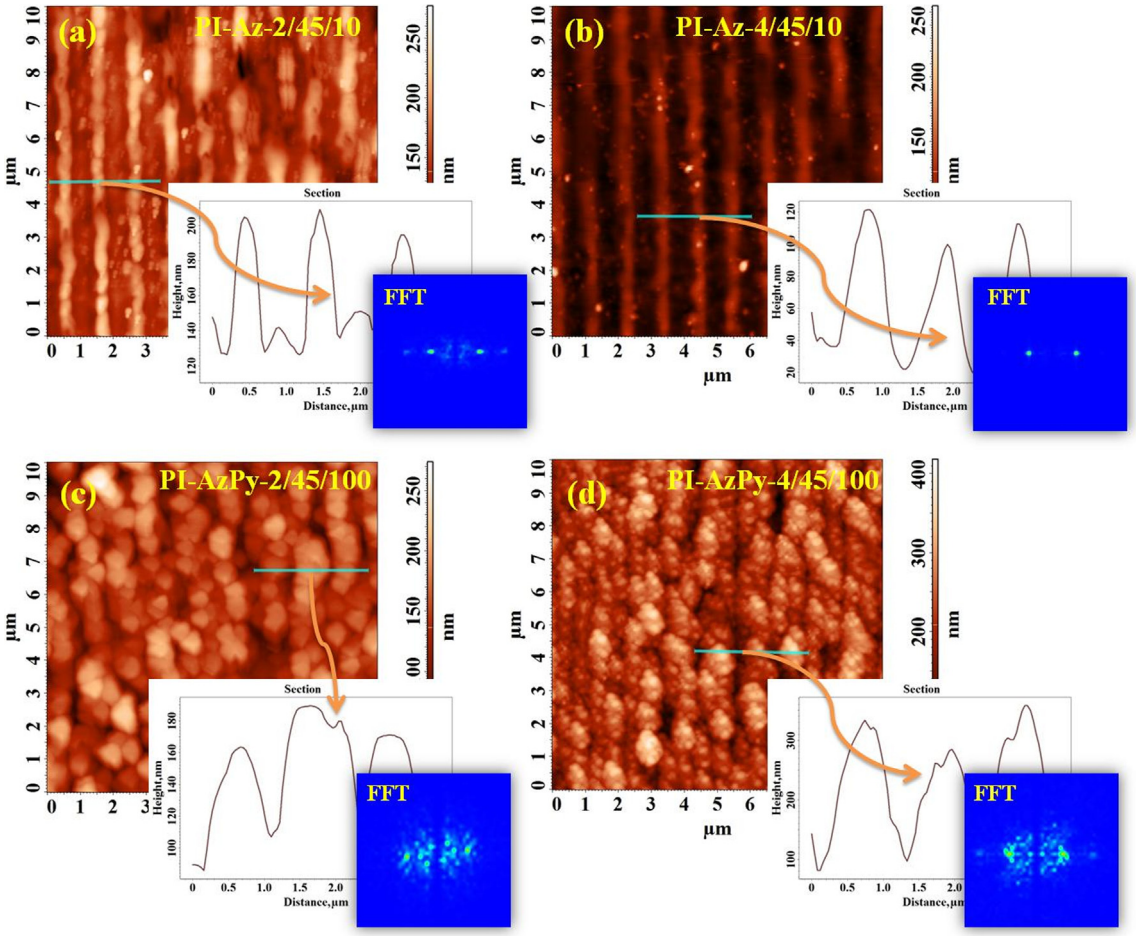

Fig. 7. Representative 2D AFM image, corresponding cross-section profiles, and fast Fourier transform (FFT) images of the SRGs obtained for (a) **PI-Az-2** and (b) **PI-Az-4** at 45 mJ/cm^2 and 10 pulses and for (c) **PI-AzPy-2** and (d) **PI-AzPy-4** at 45 mJ/cm^2 and 100 pulses.

field. So observation of the proper TN electro-optical effects could confirm the permanent uniform alignment and anchoring of the molecular director at the boundary orienting layers [57].

The photoaligning properties of **PI-Az-4** were examined in symmetric cells made from two identical substrates covered with this photosensitive material. The empty cells were filled with a nematic liquid crystal (NLC) (1892 from the Institute of Chemistry, Military University of Technology). The 1892 possesses birefringence $\Delta n = 0.19$, dielectric anisotropy $\Delta\varepsilon = 7.39$ and the temperature of the nematic-isotropic phase transition $T_{N\text{-}I} = 79.9$ °C [58]. The cell thickness was stabilized by the 5 µm thick glass spacers. To verify the NLC molecular orientation, the liquid crystal cells were placed under a polarizing microscope between crossed polarizers. Then, the white light was transmitted through this arrangement. The observed structures are shown in Fig. 8.

If no external electric field is applied to the cell, a bright-field is observed (Fig. 8A). This fact means that the twisted NLC alignment occurs because the photochromic azobenzene groups in the photoalignment layer generate planar orientation of the nematic liquid crystal molecules. Therefore nematic liquid crystal molecules align into the helical structure and rotate the polarization of incident light by 90 deg.

When the electric field is applied, LC molecules break the twisted orientation and align themselves along the field proportionally to the electric field's amplitude. As a result, a reduction in the intensity of light passing through the cell can be observed (Fig. 8B). When the external electric field is maximum, a dark field appears as a result of the perpendicularly to the substrates (homeotropic) LC molecules alignment. (Fig. 8C).

Fig. 9 shows the transmission of light as a function of the applied external electric field across twisted nematic liquid crystal cells (normally white operation mode). The experimental results show a good transmission of light and its continuous change with the applied electric field. It can be seen that the test LC cell based on **PI-Az-4** material shows a very stable curve with a low threshold electric field (about 0.28 V/µm).

Fig. 10 shows the rise times measurements. The rise time t_{ON} is defined as the time interval required to gain transmission from a level of 10% to a level of 90% of the maximum transmittance by the application of a pulse of an external electric field. The obtained maximum value of t_{ON} was 0.9 ms (1 kHz, 1.5 V/µm). Our previous work [57] showed that azopoly(ester imide) with fluor-substituent in azobenzene moieties and standard polyimide SE-130 used in the rubbing technique exhibited higher t_{ON} than **PI-Az-4**. T_{ON} were ca. 1.7 and 1.2 ms (1 kHz, 1.5 V/µm) for azopolyimide and SE-130, respectively.

In summary, **PI-Az-4** material exhibits very good orienting properties of LC molecules. Therefore, it can be successfully used in many photonic devices based on liquid crystal materials.

3. Conclusions

In the work, a series of "T-type" polyimides with derivatives of azobenzene or azopyridine was investigated. Our studies showed that the incorporation of flexible ether and ester linkages allow the preparation of materials with good solubility. The introduction of the azopyridine moieties to the polymer backbone caused the increase of

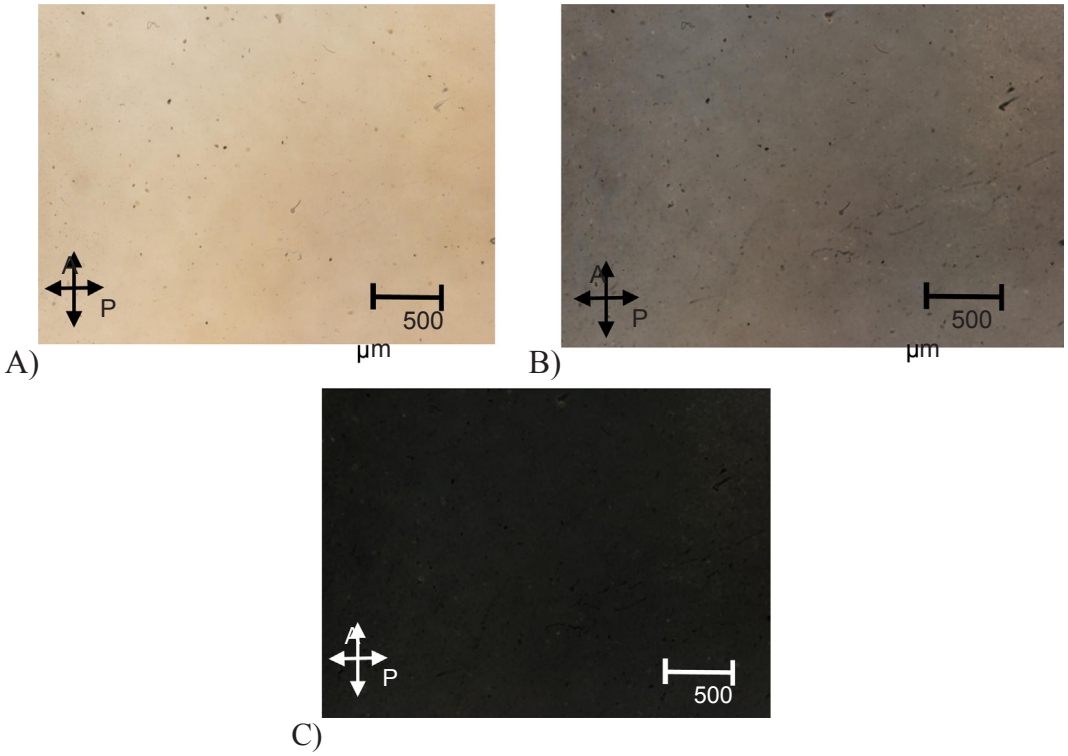

Fig. 8. Optical polarizing microscopy image of a twisted nematic cell between crossed polarizers (A) sample without applied electric field. (B) Sample with an applied electric field of the amplitude of 0,3 V/µm (100 Hz, square). C) Sample with an applied electric field of the amplitude of 1,25 V/µm (100 Hz, square).

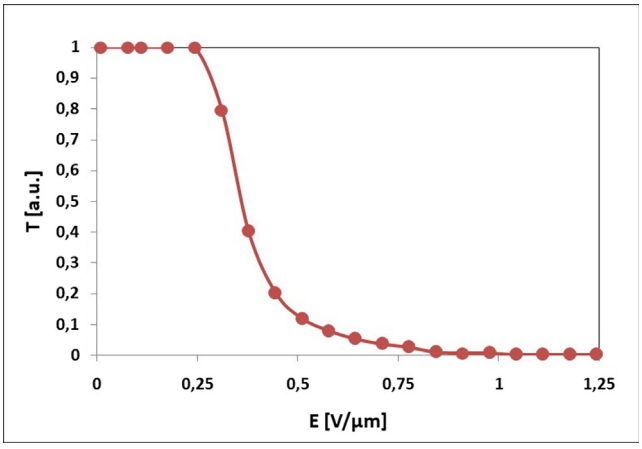

Fig. 9. Normalized light transmission as a function of the applied electric field for TN cells with photoaligned **PI-Az-4** polyimide as the alignment layers.

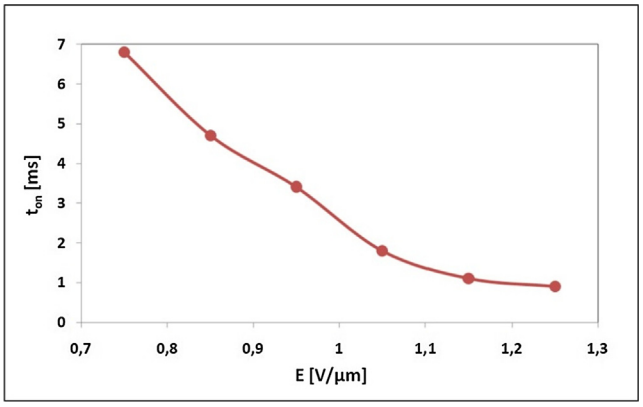

Fig. 10. Rise time for TN cells fabricated using photoalignment of the **PI-Az-4** film techniques.

the *cis-trans* isomerization of polymer films in the dark in comparison to the polyimides with azobenzene chromophores. Almost for all polyimides, the full recovery to the *trans*-form was observed within 48 h. The inscription of the SRGs was tested for all prepared azopolyimides. The modulation of SRGs depends mostly from irradiation conditions. Applied laser beam working at 45 mJ/cm^2 with 100 pulses generated the highest SRGs depths. Considering the chemical structure of polyimides, the highest SRGs modulations were achieved for polymers with a flexible aliphatic chain in the polymer backbone. Flexible main-chain can improve mass migration during the SRGs formation. Good solubility of azopolyimides allows their application as layers for the alignment of the liquid crystals. Very good orienting properties of **PI-Az-4** showed that azopolyimides may be promising materials for application in photonic devices based on liquid crystal alignment i.e. LC diffraction gratings, Fresnel lens or Vortex.

CRediT authorship contribution statement

Karolina Bujak: Investigation, Validation, Visualization, Writing - original draft. **Ion Sava:** Supervision, Writing - review & editing, Funding acquisition. **Iuliana Stoica:** Investigation, Visualization, Writing - original draft. **Vasile Tiron:** Investigation. **Ionut Topala:** Investigation, Funding acquisition. **Rafał Węgłowski:** Investigation, Visualization, Writing - original draft. **Ewa Schab-Balcerzak:** Writing - review & editing. **Jolanta Konieczkowska:** Conceptualization, Investigation, Resources, Funding acquisition, Supervision, Writing - review & editing.

Declaration of Competing Interest

The authors declare that they have no known competing financial interests or personal relationships that could have appeared to influence the work reported in this paper.

Acknowledgments

We acknowledge the support from the National Science Centre, Poland, Grant No. 2016/21/N/ST5/03037, Ministry of Research and Innovation, Romania, CNCS - UEFISCDI, Project No. PN-III-P4-ID-PCE-2016-0708, within PNCDI III and Ministry of Research and Innovation, Romania, within UAIC institutional performance Grant No. 34PFE/2018.

Appendix A. Supplementary material

Supplementary data to this article can be found online at https://doi.org/10.1016/j.eurpolymj.2020.109563.

References

[1] A. Priimagi, A. Shevchenko, Azopolymer-based micro- and nanopatterning for photonic applications, J. Polym. Sci. B: Polym. Phys. 52 (2014) 163–182, https://doi.org/10.1002/polb.23390.
[2] Y. Wu, A. Natansohn, P. Rochon, Photoinduced birefringence and surface relief gratings in polyurethane elastomers with azobenzene chromophore in the hard segment, Macromolecules 37 (2004) 6090–6095, https://doi.org/10.1021/ma0493980.
[3] F. Buchholtz, A. Zelichenok, V. Krongauz, Synthesis of new photochromic polymers based on phenoxynaphthacenequinone, Macromolecules 26 (1993) 906–910, https://doi.org/10.1021/ma00057a004.
[4] M. Irie, Diarylethenes for memories and switches, Chem. Rev. 100 (2000) 1685–1716, https://doi.org/10.1021/cr980069d.
[5] G. Berkovic, V. Krongauz, V. Weiss, Spiropyrans and spirooxazines for memories and switches, Chem. Rev. 100 (2000) 1741–1753, https://doi.org/10.1021/cr9800715.
[6] Y. Yokoyama, Fulgides for memories and switches, Chem. Rev. 100 (2000) 1717–1739, https://doi.org/10.1021/cr980070c.
[7] J.A. Delaire, K. Nakatani, Linear and nonlinear optical properties of photochromic molecules and materials, Chem. Rev. 100 (2000) 1817–1845, https://doi.org/10.1021/cr980078m.
[8] A. Natansohn, P. Rochon, Photoinduced motions in azo-containing polymers, Chem. Rev. 102 (2002) 4139–4175, https://doi.org/10.1021/cr970155y.
[9] G. Iftime, A. Natansohn, P. Rochon, Synthesis and characterization of two chiral azobenzene-containing copolymers, Macromolecules 35 (2002) 365–369, https://doi.org/10.1021/ma010477a.
[10] K.G. Yager, C.J. Barrett, All-optical patterning of azo polymer films, Curr. Opin. Sol. Stat. Mater. Sci. 5 (2001) 487–494.
[11] M. Fischer, A.E. Osman, P.-A. Blanche, M. Dumont, Photoinduce dichroism as a tool for understanding orientational mobility of photoisomerizable dyes in amorphous matrices, Synth. Met. 115 (2000) 139–144, https://doi.org/10.1016/S0379-6779(00)00335-0.
[12] C.J. Barrett, J. Mamiya, K.G. Yager, T. Ikeda, Photo-mechanical effects in azobenzene-containing soft materials, Soft Matter 2 (2007) 1249–1261, https://doi.org/10.1039/B705619B.
[13] A. Priimagi, M. Kaivola, M. Virkki, F.J. Rodriguez, M. Kauranen, Suppression of chromophore aggregation in amorphous polymeric materials: towards more efficient photoresponsive behavior, J. Nonlinear Opt. Phys. Mater. 19 (2010) 57–73, https://doi.org/10.1142/S0218863510005091.
[14] A.E.J. Wilson, Applications of photochromic polymer films, Phys. Techno1. 15 (1984) 232–238.
[15] T.J. Wigglesworth, A.J. Myles, N.R. Branda, High-Content Photochromic Polymers Based on Dithienylethenes, Eur. J. Org. Chem. 7 (2005) 1233–1238, https://doi.org/10.1002/ejoc.200400623.
[16] G.S. Kumar, D.C. Neckers, Photochemistry of azobenzene-containing polymers, Chem. Rev. 89 (1989) 1915–1925, https://doi.org/10.1021/cr00098a012.
[17] V. Shibaev, A. Bobrovsky, N. Boiko, Photoactive liquid crystalline polymer systems with light-controllable structure and optical properties, Prog. Polym. Sci. 28 (2003) 729–836, https://doi.org/10.1016/S0079-6700(02)00086-2.
[18] O.N. Oliveira Jr., D.S. dos Santos Jr., D.T. Balogh, V. Zucolotto, C.R. Mendonc, Optical storage and surface-relief gratings in azobenzene-containing nanostructured films, Adv. Colloid Interface Sci. 116 (2005) 179–192. https://doi.org/10.1016/j.cis.2005.05.008.
[19] D.H. Wang, K.M. Lee, Z. Yu, H. Koerner, R.A. Vaia, T.J. White, L.-S. Tan, Photomechanical response of glassy azobenzene polyimide networks, Macromolecules 44 (2011) 3840–3846, https://doi.org/10.1021/ma200427q.
[20] X. Meng, A. Natansohn, P. Rochon, Azo polymers for reversible optical storage. 1 1 poly{4,4'-(1-methylethylidene)bisphenylene 3-[4-(4-nitrophenylazo)phenyl]-3-azapentanedioate, J. Polym. Sci. B: Polym. Phys. 34 (1996) 1461-1466. https://doi.org/10.1002/(SICI)1099-0488(199606)34:8 < 1461::AID-POLB9 > 3.0.CO;2-V.
[21] C.-P. Yang, H.-W. Yang, Preparation and characterization of organosoluble copolyimides based on a pair of commercial aromatic dianhydride and one aromatic diamine, 1,4-Bis(4-aminophenoxy)-2-tert-butylbenzene, J. Appl. Polym. Sci. 75 (2000) 87–95, https://doi.org/10.1002/(SICI)1097-4628(20000103)75:1 < 87::AID-APP10 > 3.0.CO;2-R.
[22] O. Yaroshchuk, Y. Reznikov, Photoalignment of liquid crystals: basics and current trends, J. Mater. Chem. 22 (2012) 286–300, https://doi.org/10.1039/C1JM13485J.
[23] C.J. Barrett, A.L. Natansohn, P.L. Rochon, Mechanism of pptically inscribed high-efficiency diffraction gratings in Azo polymer films, J. Phys. Chem. 100 (1996) 8836–8842, https://doi.org/10.1021/jp953300p.
[24] K.G. Yager, C.J. Barrett, Novel photo-switching using azobenzene functional materials, J. Photochem. Photobiol. A: Chem. 182 (2006) 250–261, https://doi.org/10.1016/j.jphotochem.2006.04.021.
[25] A. Priimagi, M. Kaivola, Enhanced photoinduced birefringence in polymer-dye complexes: Hydrogen bonding makes a difference, 121103-1-121103-3, Appl. Phys. Lett. 90 (2007), https://doi.org/10.1063/1.2714292.
[26] C.-J. Chang, W.-T. Whang, C.-C. Hsu, Z.-Y. Ding, K.-Y. Hsu, S.-H. Lin, Synthesis and relationships between the nonlinear optical and holographic properties of dual functional azocarbazole chromophores based on photorefractive polymers, Macromolecules 32 (1999) 5637–5646, https://doi.org/10.1021/ma981922d.
[27] S. Kawata, Y. Kawata, Three-dimensional optical data storage using photochromic materials, Chem. Rev. 100 (2000) 1777–1788, https://doi.org/10.1021/cr980073p.
[28] S.K. Yeshodha, C.K.S. Pillai, N. Tsustsumi, Stable polymeric materials for nonlinear optics: a review based on azobenzene systems, Prog. Polym. Sci. 29 (2004) 45–74, https://doi.org/10.1016/j.progpolymsci.2003.07.002.
[29] D. Wang, X. Wang, Amphiphilic azo polymers: molecular engineering, self-assembly, and photoresponsive properties, Prog. Polym. Sci. 38 (2013) 271–301, https://doi.org/10.1016/j.progpolymsci.2012.07.003.
[30] Y. Wu, J. Mamiya, A. Kanazawa, T. Shiono, T. Ikeda, Q. Zhang, Photoinduced alignment of polymer liquid crystals containing azobenzene moieties in the side chain. 6. biaxiality and three-dimensional reorientation, Macromolecules 32 (1999) 8829–8835, https://doi.org/10.1021/ma9903052.
[31] T.J. White, N.V. Tabiryan, S.V. Serak, U.A. Hrozhyk, V.P. Tondiglia, H. Koerner, R.A. Vaia, T.J. Bunning, A high frequency photodriven polymer oscillator, Soft Matter 4 (2008) 1796–1798, https://doi.org/10.1039/B805434G.
[32] Z. Sekkat, J. Wood, W. Knoll, Reorientation mechanism of azobenzenes within the trans → cis photoisomerization, J. Phys. Chem. 99 (1995) 17226–17234, https://doi.org/10.1021/j100047a029.
[33] J. Konieczkowska, E. Schab-Balcerzak, M. Libera, I. Mihaila, I. Sava, Surface relief gratings in azopolyimides induced by pulsed laser irradiation, Eur. Polym. J. 110 (2019) 85–89, https://doi.org/10.1016/j.eurpolymj.2018.11.022.
[34] E. Schab-Balcerzak, J. Konieczkowska, M. Siwy, A. Sobolewska, M. Wojtowicz, M. Wiacek, Comparative studies of polyimides with covalently bonded azo-dyes with their supramolecular analoges: Thermo-optical and photoinduced properties, Opt. Mater. 36 (2014) 892–902, https://doi.org/10.1016/j.optmat.2013.12.017.
[35] K. Bujak, H. Orlikowska, J.G. Małecki, E. Schab-Balcerzak, S. Bartkiewicz, J. Bogucki, A. Sobolewska, J. Konieczkowska, Fast dark cis-trans isomerization of azopyridine derivatives in comparison to their azobenzene analogues: Experimental and computational study, Dyes Pigm. 160 (2019) 654–662, https://doi.org/10.1016/j.dyepig.2018.09.006.
[36] K. Bujak, H. Orlikowska, A. Sobolewska, E. Schab-Balcerzak, H. Janeczek, S. Bartkiewicz, J. Konieczkowska, Azobenzene vs azopyridine and matrix molar masses effect on photoinduced Phenomena, Eur. Polym. J. 115 (2019) 173–184, https://doi.org/10.1016/j.eurpolymj.2019.03.028.
[37] J. Konieczkowska, E. Schab-Balcerzak, M. Siwy, K. Switkowski, A. Kozanecka-Szmigiel, Large and highly stable photoinduced birefringence in poly(amideimide)s with two azochromophores per structural unit, Opt. Mater. 39 (2015) 199–206, https://doi.org/10.1016/j.optmat.2014.11.026.
[38] A. Kozanecka-Szmigiel, J. Konieczkowska, D. Szmigiel, J. Antonowicz, J. Małecki, E. Schab-Balcerzak, Blue-light-induced processes in a series of azobenzene poly (ester imide)s, J. Photochem. Photobiol. A: Chem. 347 (2017) 177–185, https://doi.org/10.1016/j.jphotochem.2017.07.047.
[39] I. Sava, A.-M. Resmerita, G. Lisa, V. Damian, N. Hurduc, Synthesis and photochromic behavior of new polyimides containing azobenzene side groups, Polymer 49 (2008) 1475–1482, https://doi.org/10.1016/j.polymer.2008.02.004.
[40] A. Kozanecka-Szmigiel, J. Konieczkowska, D. Szmigiel, K. Switkowski, M. Siwy, P. Kuszewski, E. Schab-Balcerzak, Photoinduced birefringence of novel azobenzene poly(esterimide)s; the effect of chromophore substituent and excitation conditions, Dyes Pigm. 114 (2015) 151–157, https://doi.org/10.1016/j.dyepig.2014.11.007.
[41] E. Schab-Balcerzak, M. Siwy, B. Jarzabek, A. Kozanecka-Szmigiel, K. Switkowski, B. Pura, Post and prepolymerization strategies to develop novel photochromic poly (esterimide)s, J. Appl. Polym. Sci. 120 (2011) 631–643, https://doi.org/10.1002/app.33202.
[42] N. Nemoto, F. Miyata, Y. Nagase, J. Abe, M. Hasegawa, Y. Shirai, Novel Types of polyesters containing second-order nonlinear optically active chromophores with high density, Macromolecules 29 (1996) 2365–2371, https://doi.org/10.1021/ma951032n.
[43] K. Bujak, K. Nocoń, A. Jankowski, A. Wolińska-Grabczyk, E. Schab-Balcerzak, H. Janeczek, J. Konieczkowska, Azopolymers with imide structures as light-switchable membranes in controlled gas separation, Eur. Polym. J. 118 (2019) 186–194, https://doi.org/10.1016/j.eurpolymj.2019.05.051.
[44] J. Konieczkowska, A. Kozanecka-Szmigiel, W. Piecek, R. Węgłowski, E. Schab-Balcerzak, Azopolyimides – influence of chemical structure on azochromophore photo-orientation efficiency, Polimery 63(7-8) (2018) 481–487 http://dx.doi.org/10.14314/polimery.2018.7.1.
[45] A. Bhatnagar, J. Mueller, D.J. Osborn, T.L. Martin, J. Wirtz, D.K. Mohanty, Azoaromatic polyethers, Polymer 36 (1995) 3019–3025, https://doi.org/10.1016/0032-3861(95)94353-U.
[46] I. Sava, L. Sacarescu, I. Stoica, I. Apostol, V. Damian, N. Hurduc, Photochromic properties of polyimide and polysiloxane azopolymers, Polym. Int. 58 (2009) 163,

https://doi.org/10.1002/pi.2508.
[47] X. Jiang, X. Chen, X. Yue, J. Zhang, S. Guan, H. Zhang, W. Zhang, Q. Chen, Synthesis and characterization of photoactive poly(arylene ether sulfone)s containing azobenzene moieties in their main chains, React. Funct. Polym. 70 (2010) 616–621, https://doi.org/10.1016/j.reactfunctpolym.2010.05.007.
[48] P. Arab, E. Parrish, T. İslamoğlu, H.M. El-Kaderi, Synthesis and evaluation of porous azo-linked polymers for carbon dioxide capture and separation, J. Mater. Chem. A 3 (2015) 20586–20594, https://doi.org/10.1039/C5TA04308E.
[49] J. García-Amorós, D. Velasco, Recent advances towards azobenzene-based light-driven real-time information-transmitting materials, Beilstein J. Org. Chem. 8 (2012) 1003–1017, https://doi.org/10.3762/bjoc.8.113.
[50] I. Stoica, E.G. Hitruc, D. Timpu, V. Barboiu, D.S. Vasilescu, Establishing proper scanning conditions in atomic force microscopy on polyimide and polyurethane samples and their effect on 3D surface texture parameters, Scanning 37 (5) (2015) 335–349, https://doi.org/10.1002/sca.21216.
[51] C. Hubert, C. Fiorini-Debuisschert, I. Maurin, J.M. Nunzi, P. Raimond, Spontaneous patterning of hexagonal structures in an azo-polymer using light-controlled mass transport, Adv. Mater. 14 (2002) 729–732.
[52] S. Savić Sević, D. Pantelić, Biopolymer holographic diffraction gratings, Opt. Mater. 30 (2008) 1205–1207.
[53] I. Stoica, L. Epure, I. Sava, V. Damian, N. Hurduc, An atomic force microscopy statistical analysis of laser-induced azo-polyimide periodic tridimensional nanogrooves, Microsc. Res. Techn. 76 (9) (2013) 914–923, https://doi.org/10.1002/jemt.22248.
[54] C. Fiorini, N. Prudhomme, G. de Veyrac, I. Maurin, P. Raimond, J.-M. Nunzi, Molecular migration mechanism for laser-induced surface relief grating formation, Synth. Met. 115 (2000) 121–125, https://doi.org/10.1016/S0379-6779(00)00332-5.
[55] X. Wu, T.T.N. Nguyen, I. Ledoux-Rak, C.T. Nguyen, N.D. Lai, Optically accelerated formation of one- and two-dimensional holographic surface relief gratings on DR1/PMMA, in: Emilia Mihaylova (Ed.), Holography – Basic Principles and Contemporary Applications, IntechOpen Published, London, May 29th 2013, pp. 147–170, https://doi.org/10.5772/53788.
[56] S. Moujdi, A. Rahmouni, T. Mahfoud, D.V. Nesterenko, M. Halim, Z. Sekkat, Surface relief gratings in azo-polymers revisited, J. Appl. Phys. 124 (2018) 213103, https://doi.org/10.1063/1.5058746.
[57] R. Węgłowski, W. Piecek, A. Kozanecka-Szmigiel, J. Konieczkowska, E. Schab-Balcerzak, Poly(esterimide) bearing azobenzene units as photoaligning layer for liquid crystals, Opt. Mater. 49 (2015) 224–229, https://doi.org/10.1016/j.optmat.2015.09.020.
[58] R. Mazur, W. Piecek, Z. Raszewski, P. Morawiak, K. Garbat, O. Chojnowska, M. Mrukiewicz, M. Olifierczuk, J. Kedzierski, R. Dabrowski, D. Węgłowska, Nematic liquid crystal mixtures for 3D active glasses application, Liq. Cryst. 44 (2017) 417–426.